Proceedings of ASME Turbo Expo 2011
GT2011
June 6-10, 2011, Vancouver, British Columbia, Canada

GT2011-46351

HEAVY-DUTY GAS TURBINES AXIAL THRUST CALCULATION IN DIFFERENT OPERATING CONDITIONS

Luca Bozzi*, Francesco Malavasi
Ansaldo Energia
Product Development Engineering
Turbomachinery
Via Nicola Lorenzi, 8
16152 Genoa (Italy)
luca.bozzi@aen.ansaldo.it

Valeria Garotta
CFD Engineering S.r.l.
Industry Division
Piazza della Vittoria 7/2A,
16121 Genoa (Italy)
garotta@cfd-engineering.it

ABSTRACT

Several types of forces give a contribution to the axial thrust of gas turbines shafts: flow-path forces (due to blades, endwalls and shrouds of compressor and turbine rows), forces acting on the surfaces of rotor-stator cavities, disks forces (due to the different pressure levels in the rotating cavities inside the rotor), etc. As a rule, the estimation of the rotor thrust needs the handling of a large amount of output data, resulting from different codes.

This paper presents a calculation tool to estimate the rotor axial thrust from the results of compressor, turbine and secondary air system calculations. Applications to heavy-duty gas turbines of different classes and sizes (namely two models of AEx4.3A F-class family, AE64.3A and AE94.3A, and the AE94.2 E-class gas turbines) are presented. On the basis of calculation results, in base load and part load operating conditions, guidelines to determine the rules of variation of axial bearing thrust and the relating scatter band are given.

Pressure transducers were installed on the bearing pads of different gas turbines, in order to provide experimental data for the calibration of the calculation procedure. Comparison of experimental data with numerical results proves that the proposed calculation tool properly evaluates gas turbines rotor thrust and the axial bearing load.

NOMENCLATURE

A	area of rotor component surfaces;	mm^2
BL15	base load reference condition, 100% IGV, +15C ambient temperature;	-
BL-15	base load condition, 100% IGV, -15C ambient temperature;	-
BL45	base load condition, 100% IGV, +45C ambient temperature;	-
BLC	compressor blade/endwall forces output file;	-
BLT	turbine blade/endwall forces output file;	-
BT	bearing thrust (net axial load on compressor bearing, including the thrust piston relief);	kN
c	bearing thrust off-set coefficient;	kN
CMP	compressor calculation output file;	-
CST	compressor stage;	-
D2	subsystem index (2nd disk);	-
Ex	external extraction line "x"	-
Exi	inner extraction line "x"	-
FSNL	idle condition, 15C ambient temperature;	-
IGV	compressor Inlet Guide Vanes;	
k	rotor thrust gradient;	kN/bar
LAB	surface type index (left disk surface);	-
m	bearing thrust gradient;	kN/bar
$\dot{m}$	compressor mass flow;	kg/s
$\dot{m}_0$	compressor mass flow in base load reference condition (100% IGV and +15C);	kg/s
ML15	partial load, closed IGV, +15C ambient temperature;	-
p	pressure;	bar
P	power output;	MW
p_{out}	compressor discharge pressure;	bar
PL	measured axial load on a single bearing pad;	kg
P.R.	turbine pressure ratio	-
RT	rotor axial thrust due to rotor components (excluding the thrust piston relief);	kN
S BLD	blade axial force;	-

* Address all correspondence to this author.

S PR	pressure axial force;	-
S RIP	axial thrust when all rotor components are subject to atmospheric pressure;	-
S TOT	balance of pressure and blade axial forces;	-
SAS	secondary air system;	-
SASAC	secondary air system Ansaldo Code;	-
SPL	thrust index for surface subject to negative axial thrust (towards compressor air intake);	-
SPR	thrust index for surface subject to positive axial thrust (towards turbine exhaust diffuser);	-
SRCC	stator-Rotor Cavity Code;	-
TBx	SAS output file name for the cooled rotating stage “x”;	-
TUR	turbine calculation output file;	-
x	relative position of the rotor with respect to the bearing casing by a proximity sensor;	mm
z	rotor thrust off-set coefficient;	kN

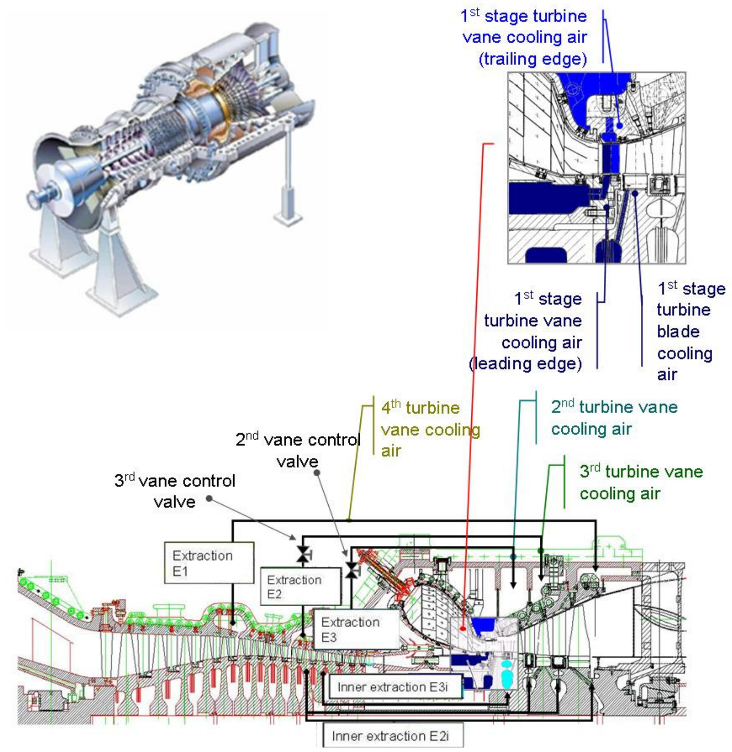

Figure 1 - AE94.3A gas turbine and cross section of secondary air system layout.

Thermodynamic data ISO base load	AE64.3A	AE94.2	AE94.2K	AE94.3A
Turbine inlet temp. acc. to ISO 2314 [°C]	1190	1075	1060	1250
Pressure ratio [-]	16,7	11,9	12,0	18,2
Power output at gen. term. [MW]	75	170	170	294
Efficency at gen term. [%]	35,9	34,9	36,5	39,7
Exhaust gas mass flow [kg/s]	213	537	540	702
Exhaust gas temperature [°C]	574	541	545	580

Table 1 - Performance data of Ansaldo gas turbines.

INTRODUCTION

In the framework of an independent power generation market, several gas turbine plants, originally designed to operate mainly close to the base load condition, need flexible and profitable operation into the dispatch and ancillary energy service market. Operating the gas turbines intermittently, quickly ramping up and down and at the lowest turndown load, when the power demand is low, represents extreme off-design conditions for engines designed for base load condition. This is the reason why several verifications on different engine components are required, in order to guarantee to plant operators the same levels of reliability and availability as in base load operating mode.

In these circumstances, besides the standard design verifications for the hot gas section, further investigations are required for other components, such as compressor and turbine bearings. Focus of this work is the thrust bearing, which sustains the rotor axial thrust produced by the engine.

Several types of forces give a contribution to the axial thrust of gas turbine shafts: flow-path forces (due to blades, endwalls and shrouds of compressor and turbine rows), forces acting on the surfaces of rotor-stator cavities, disk forces (due to different pressure levels in the rotating cavities inside the rotor).

As a rule, the estimation of the rotor thrust needs the handling of a large amount of output data, resulting from different codes. Typically, 3D Navier-Stokes tools or through-flow codes provide the flow-path forces, while a 1D fluid network solver gives the pressure levels in the turbine wheel-spaces and in the rotating passages of the secondary air system.

This paper presents a calculation tool to estimate the rotor axial thrust from the results of compressor, turbine and secondary air system calculations. Applications to heavy-duty gas turbines of different classes and sizes (see Table 1, namely two models of AEx4.3A F-class family, AE64.3A and AE94.3A, and the AE94.2 E-class gas turbines) are presented. The variation of axial thrust with load and ambient condition is presented, with reference in particular to AE94.3A units (see Figure 1).

Pressure transducers were installed on the bearing pads of different gas turbines, in order to provide experimental data for the calibration of the calculation procedure. Comparison of experimental data with numerical results is discussed.

On the basis of calculation results and experimental data, guidelines to determine the rules of variation of axial bearing thrust and the relating scatter band are given, in base load and part load operating conditions.

ROTOR OF AEx4.3A AND AE94.2 GAS TURBINES

AEx4.3A and AE94.2 heavy-duty gas turbines are single-casing and single-shaft engines for which compressor and turbine, the main components, have a common rotor. It is a disk-type rotor held up by a pre-stressed central tie-rod. Rotor disks are splinted together by radial facial serrations named as Hirth-couplings, which connect adjacent disks permitting the

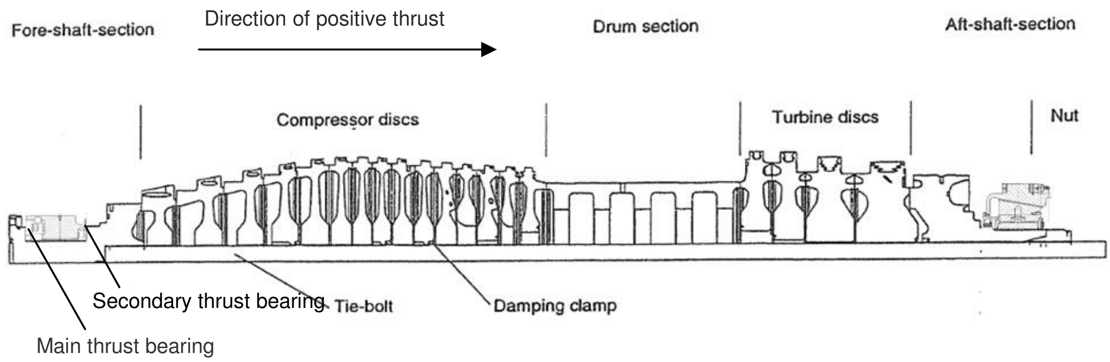

Figure 2 – Rotor of AE94.3A heavy-duty gas turbine

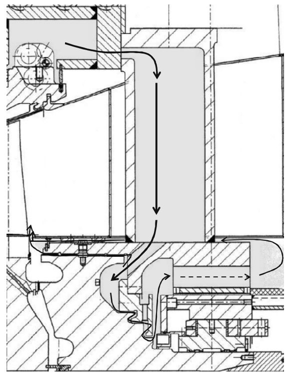

Figure 3: Thrust piston

transmission of turbine torque to the compressor (Figure 2), [1] and [2]. This rotor configuration results in a self-supporting drum of great stiffness with a high critical speed and a relatively low weight. Moreover, this configuration permits the rotor parts to be bathed in air from all sides, both in the turbine section (thanks to blade cooling air) and even in the compressor section. In particular, compressor disk assembly is split into three different blocks by three damping elements (4^{th}, 8^{th} and 10^{th} disk in Figure 2). Leakage air enters the teeth gap between the last two disks of each block and exits from the upstream coupling gaps. Thus, rotor components are warmed and cooled by circulation of air through cooling air passages and Hirth teeth gaps. Circulation of air makes rapid and more uniform the disk and tie-rod temperature changes preventing thermal stresses and rotor distortion during load changes and rapid starts, [1].

Going into details of secondary air system, a portion of air bled off from the main flow at the end of the compressor is, then, fed through bores in the center hollow shaft to the first stage blades, [3] and [4]. Furthermore, in AEx4.3A gas turbines, two additional flows inside the rotor supply cooling air for other rotating stages. The cooling air for the turbine blades of stages 2, 3 and 4 is extracted upstream of the 11^{th} and 13^{th} compressor stage and led through two different passages in the central hollow shaft (Figure 1), [2]. The cooling air is driven, by centrifugal and pressure force, towards the cavities between the turbine rotor disks, to reach, through radial bores, the rotor cascades. Cooling air, which enters the hot gas main stream, envelops the rotor hub in a film of cooling air. Turbine blades are cooled by a combination of film and convection cooling.

Journal and Thrust Bearings

The rotor is supported by two journal bearings, located outside the pressurized region. This solution ensures excellent running qualities and constant proper alignment.

As an example, Figure 3 shows a section of the exhaust casing of the turbine journal bearing for the AE94.3A GT. The casing comprises a rigid, one-piece cylinder, which supports the turbine journal bearing. Struts directly link the hub to the outer casing. The exhaust casing connects the turbine stationary vane carrier to the exhaust gas diffuser (the turbine bearing can be removed axially on the diffuser side).

In Ansaldo gas turbines, the front bearing casing (on the compressor side) contains the combined journal and thrust bearings. The casing is fixed to a ring that rests on two supports by means of radial struts guiding the airflow entering the compressor (Figure 1). The rotor can be removed without dismantling the intake shaft. In the front bearing casings are mounted two thrust bearings: the main bearing that sustains the axial thrust directed towards the turbine exhaust diffuser, and the secondary bearing that sustains the thrust directed to the compressor air intake, which can occur during the start-up phase. Figure 2 shows the annular surfaces (in the cavity shaped in the fore shaft-section) where pads of main and secondary axial bearings act.

AEx4.3A and AE94.2 gas turbines make use of modular tilting pad thrust bearings. Figure 4 shows details of AE96.3A main axial bearing which consists of ten thrust pads supported in a cage ring. Each pad is loosely retained by pad stops so that each pad is free to tilt and it is supported on a system of levers in order to equalize load sharing between the pads.

The bearings are designed to be lubricated by a pressurized oil system, with oil supplied into the cage ring annular groove. The oil then feeds from the annulus to the thrust bearing chamber via a number of radial holes in the cage ring. The thrust pads are normally manufactured from steel lined with a tin based whitemetal.

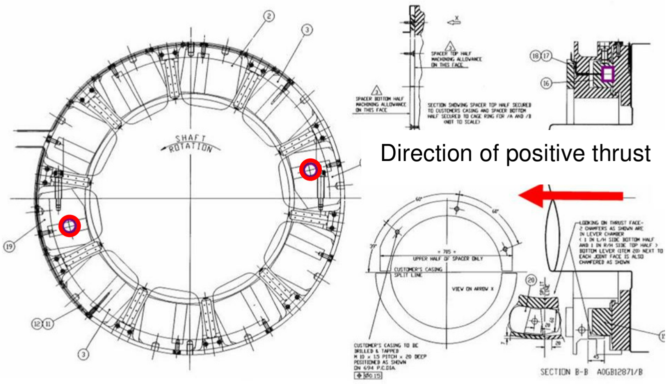

Figure 4 – Tilting pads of AE64.3A main thrust bearing (locations of pressure transducers are highlighted).

Note that the external bleed, which supplies the fourth stage vanes and the sealing air of the turbine bearing (Figure 1), ensures the proper pressure level of the thrust piston (Figure 3). The piston concurs to relieve the axial bearing of part of the axial load given by the rotor thrust. To this aim, a cavity is shaped between the rear hollow shaft and the inner part of the bearing casing. Sealing air of the turbine bearing is drawn in the cavity throughout the passages in the casing struts.

ROTOR AXIAL THRUST CALCULATION CODE

RAT code is a numerical tool in Fortran language in-house developed by Ansaldo Energia in cooperation with CFD-Engineering. The code computes the axial thrust due to air and/or gas pressure acting on rotor surfaces.

RAT acquires geometry data, pressure values along the rotor and compressor/turbine blade thrust from a few files properly formatted. The code returns the rotor thrust and the net load on the main and secondary bearings.

Calculation method

The rotor axial thrust is evaluated as the algebraic sum of the values calculated for each rotor component of Figure 2. To this aim, the gas turbine rotor is divided into five main components/sections (Figure 5); namely compressor, turbine, fore hollow shaft, central hollow shaft (the drum section) and aft/rear hollow shaft. Every rotor component is, in its turn, discretized in subsystems. For instance, the component "*compressor*" is divided in n subsystems, corresponding to compressor disks. Note that the components representing the hollow shafts consist of a single subsystem. Finally each subsystem is discretized in several surfaces.

RAT computes the axial thrust on every surface of a single subsystem. Then, the subsystem balance results as an algebraic sum of the values calculated for each of its surfaces.

Similarly, the thrust balance for a single component is performed after calculating the axial thrust for all the subsystems belonging to that component. Finally, the rotor axial thrust is obtained as a sum of the values calculated for each component.

A rigorous codifying procedure of subsystems and surfaces allows associating a correct pressure value for every surface. In particular, with reference to Figure 6, identification strings, consisting of ten characters, allow the code identify the portion of output file (deriving from compressor, turbine and SAS calculations) where to read the proper value of static pressure. All strings are collected into a file, named set-up file, which defines the links between component surfaces and calculated pressures.

Input data files

The axial thrust results from a balance of different forces:

- Flow-path forces
  - Blade forces
  - Endwall forces
- Pressure forces
  - Disk forces (due to the different pressure levels in rotating cavities inside the rotor)
  - Rotor-stator cavities forces

The code computes the rotor axial thrust starting from a set of fluid-dynamic and geometrical data. In particular, the pressure values, required to calculate the forces acting on rotor components, derive from the following calculations.

- Flow-path forces:
  - 3D Navier-Stokes and/or 2D through-flow calculations of compressor and turbine section;
  - gas turbine thermal balance;
- Pressure forces:
  - 1D calculation of pressure losses in the rotating passages of secondary air system.

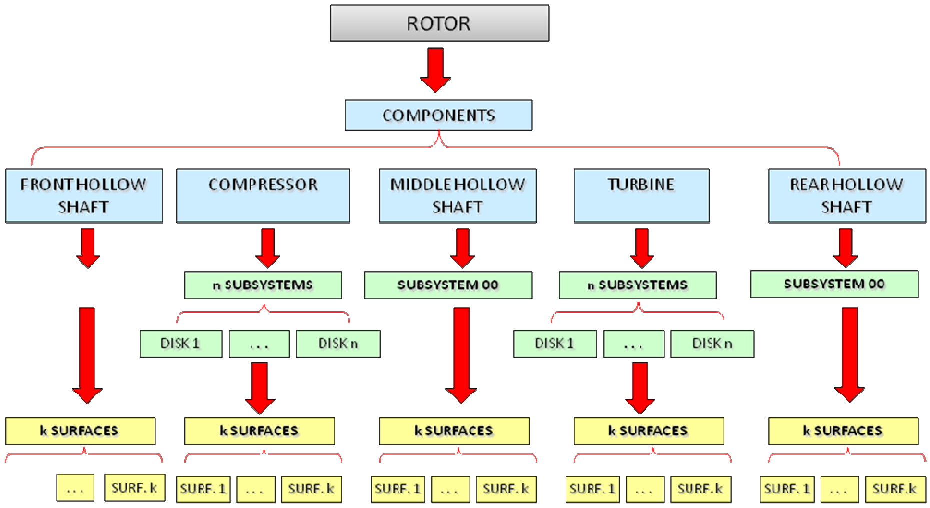

Figure 5 – Flow diagram for calculation of axial forces on rotor components.

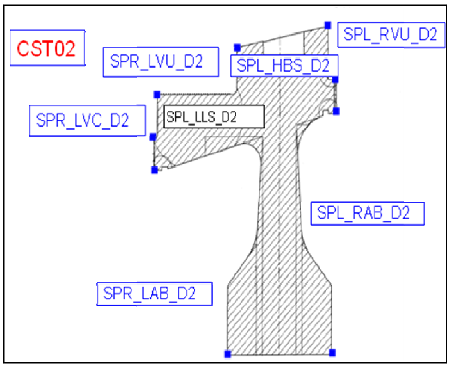

Figure 6 – Split of coded surfaces for AE94.3A 2nd compressor disk.

Geometrical data are recorded in a GEO file that mainly contains the inner and outer radius, in hot conditions, of every surface concurring to the axial thrust. The secondary air system calculation plays a fundamental role in the evaluation of axial thrust since the pressure levels in the rotor sections are given by the SAS code (SASAC). It is a modular 1D tool able to model the entire fluid network of the secondary air system, from the compressor extraction points to the hot gas section. Loss elements are modeled by equations based on literature standard methods (such as [5]) and calibrated on Ansaldo gas turbine geometry. SAS code is coupled to the Stator Rotor Cavity Code (SRCC, [6]), which is a specific program for studying the engine sealing system. The coupled SASAC/SRCC air system simulation enables the estimation of the averaged pressure level acting on the rotating surfaces of stator-rotor cavities, [7].

Set-up file

The rotor discretization in components, subsystems and surfaces is reported in a Set-up File (Figure 7). In particular, the file contains, for each component, the list of all its subsystems; for each subsystem, the list of surfaces in which it is divided. The main routine reads row by row the Setup File and, after loading geometry data, computes the axial thrust acting on the examined surface. Note that geometry data are firstly checked by a routine that verifies that no net axial thrust (S RIP, Figure 8) exists when all the rotor components are subject to atmospheric pressure. Small values of S RIP are admitted, which are due to approximations of geometry data.

As an example, referring to Figure 7, the string SPR_LAB_D1 identifies the first surface of the subsystem CST01 (compressor disk of the 1st stage). The thrust index SPR states that the surface is subject to a positive axial thrust (directed towards the turbine exhaust diffuser), LAB is the surface type index, and D1 is the subsystem index. Note that the acronym for the surface, LAB_D1, is crucial for the attribution of the correct pressure value. In this case the character D1 makes the code routine read the part of calculated data relating to the 1st stage in the compressor output file. Starting from these values, the string LAB makes the code calculate the pressure acting on the left surface of the disk located below the Hirth coupling.

The second column of the Setup File reports the acronym that identifies the fluid-dynamic data files used to compute the pressure value acting on the surface. For compressor and turbine calculation output files, acronyms CMP and TUR are used; whereas for SAS results the file name indicates the cooled rotating stage (for example TBx). Flow path forces, namely forces on blades and endwalls, are acquired from specific files (BLC for compressor section and BLT for turbine section) which report axial thrust on blades and endwalls calculated by 3D Navier-Stokes or 2D through-flow calculations.

The third column of the Setup Data File hosts an auxiliary datum, used when the pressure value is acquired from SASAC outputs. It indicates the element number in the fluid-network.

The fourth column may possibly indicate a calibration coefficient for the pressure value. Finally, the fifth column can be used to explicitly specify a numeric value of pressure.

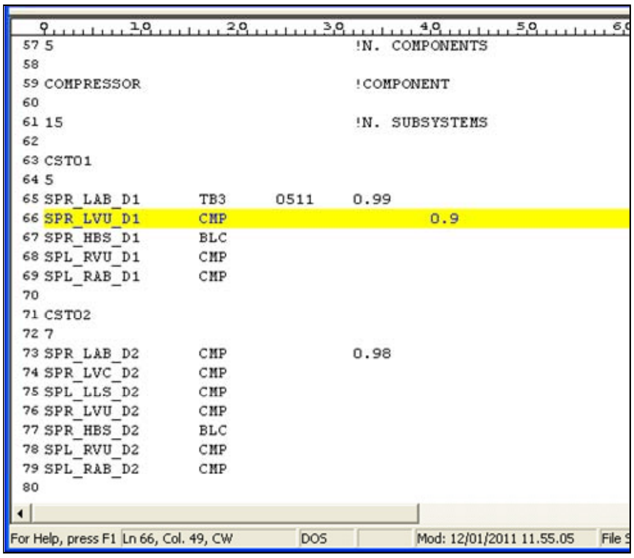

```
57 5                                  !N. COMPONENTS
58
59 COMPRESSOR                         !COMPONENT
60
61 15                                 !N. SUBSYSTEMS
62
63 CST01
64 5
65 SPR_LAB_D1     TB3     0511     0.99
66 SPR_LVU_D1     CMP                       0.9
67 SPR_HBS_D1     BLC
68 SPL_RVU_D1     CMP
69 SPL_RAB_D1     CMP
70
71 CST02
72 7
73 SPR_LAB_D2     CMP              0.98
74 SPR_LVC_D2     CMP
75 SPL_LLS_D2     CMP
76 SPR_LVU_D2     CMP
77 SPR_HBS_D2     BLC
78 SPL_RVU_D2     CMP
79 SPL_RAB_D2     CMP
80
For Help, press F1   Ln 66, Col. 49, CW   DOS   Mod: 12/01/2011 11.55.05
```

Figure 7 – Section of the set-up file.

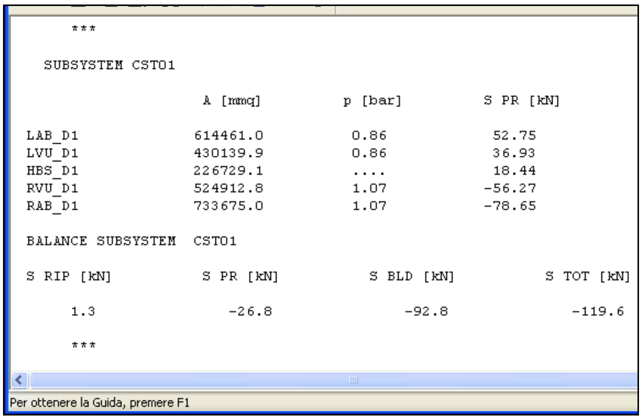

```
***

SUBSYSTEM CST01

                A [mmq]        p [bar]        S PR [kN]

LAB_D1          614461.0       0.86           52.75
LVU_D1          430139.9       0.86           36.93
HBS_D1          226729.1       ....           18.44
RVU_D1          524912.8       1.07          -56.27
RAB_D1          733675.0       1.07          -78.65

BALANCE SUBSYSTEM  CST01

S RIP [kN]      S PR [kN]      S BLD [kN]      S TOT [kN]

1.3             -26.8          -92.8           -119.6

***
Per ottenere la Guida, premere F1
```

Figure 8 – Results for the 1st compressor disk sub-system.

Calibration coefficients

Calibration coefficients can be used for tuning. Usually coefficients are used to correct pressure values computed by SAS code, which, as already stated, gives an average value in the rotating passages [7]. Such calibration coefficients have been deduced both by CFD analysis of air flow in multi-disk type rotor ([8] and [9]) and by comparison of calculated bearing thrust with experimental data.

Rotating cavities interested by secondary air flow usually give a small positive net contribution to rotor axial thrust, due to the different outer radius of compressor and turbine disks. Results suggest that a tuning coefficient of 0.85, applied to pressure values calculated for rotating cavities below the Hirth couplings, is precautionary for AEx4.3A engines. Calibration, in fact, gives a +10% extra contribution to axial bearing thrust.

Furthermore, rotating surfaces of certain wheel spaces are crucial for thrust calculation. In particular, the pressure level has to be carefully evaluated for the turbine stator-rotor cavities that are not balanced by adjacent cavities (or by cavities in the compressor side having corresponding radii), such as for the 1st stage rim cavity (Figure 9). With reference to AE94.3A gas turbine, note that a 10% error in pressure evaluation on the highlighted surface in Figure 9, drives a 40% error in the computation of the net axial thrust. As well known, the pressure level in such cavity is strongly influenced by radial clearances in hot conditions used by the SAS code. In this case a safe coefficient of 1.05 should be used.

Finally, field measurements, if available, can also be used to correct pressure values. That's the case of the pressure level acting on the thrust piston cavity, which is monitored in some engines. Field data suggest a reduction coefficient of 0.95 applied to pressure calculated by SAS code.

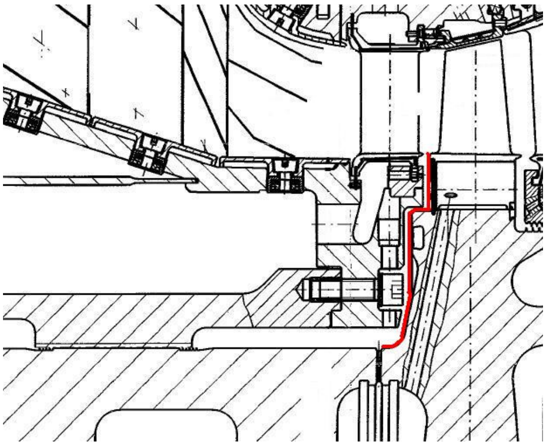

Figure 9 – Sketch of the 1° stage rim cavity of AE94.3A GT.

Output data

The structure of the output file follows closely the set-up file. Area, pressure and calculated axial thrust for each subsystem are reported according to the surfaces list. Figure 8 shows that, before going on to the following subsystem, a balance is reported that shows the axial thrust in switch-off conditions S_RIP (atmospheric pressure acting everywhere), the axial thrust due to inter-disc and stator-rotor cavities (S PR), the axial thrust due to blade flow-path forces (S BLD) and the net axial thrust on the subsystem (S TOT). The same balance is shown for the section/main component and for the entire rotor.

The file is concluded by a summary that reports the axial thrust on every component, the thrust piston contribution, and the rotor thrust, RT, which corresponds to the bearing thrust, BT, in case of depressurization of the bleed line for the thrust piston (pressure equals to atmospheric level).

Figures 10 and 11 show the bar plots of a typical results summary for the AE94.3A gas turbine. Separate contributions for pressure forces, flow-path forces and thrust piston are reported in Figure 10, together with the net bearing load BT and the rotor trust RT. The output file also allows for investigating the load distribution by component. Typically, the axial thrust on compressor (negative) and turbine (positive) are of the order of ten times the bearing thrust, BT, as shown in Figure 11. Hence, 10% errors in the computation of the axial thrust on compressor or turbine components, can lead to errors up to 100% in the evaluation of the bearing thrust BT. Thus, it's crucial to calibrate the calculation procedure on the basis of experimental data.

Furthermore, Figure 11 suggests that, since the main contributions to bearing thrust arise from compressor and turbine components, if the axial thrust on compressor section is higher than the one on the turbine section, as typically happens during initial start-up, the bearing thrust BT can be negative, i.e. directed towards the air intake.

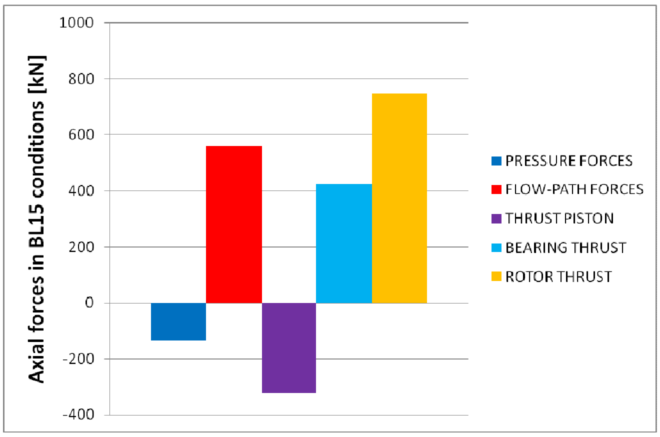

Figure 10 – Thrust calculation results for AE943A gas turbine in base load conditions.

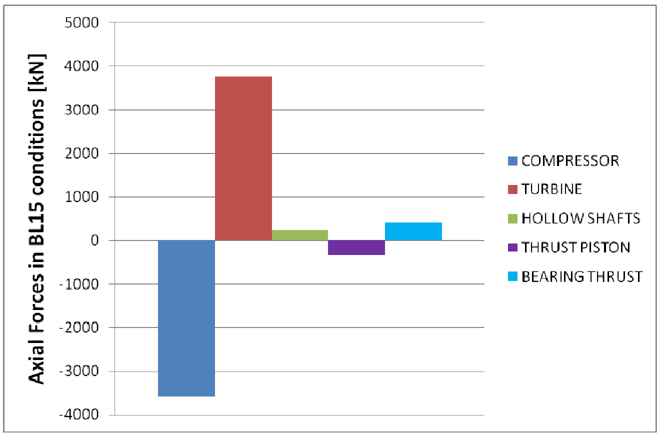

Figure 11 – Axial thrust distribution by rotor component for AE943A gas turbine in base load conditions.

APPLICATION TO AE94.3A GAS TURBINE

In this example, axial thrust calculations were performed for AE94.3A gas turbine in different ambient and load conditions. Figure 12 shows the rotor thrust, RT (the axial thrust in case of depressurized thrust piston) as a function of compressor end pressure.

Calculation results in different operating conditions point out that, as expected, the rotor thrust RT grows linearly with the pressure level of the gas turbine engine.

Figure 13 shows the net thrust, *BT*, on the main axial bearing (hence considering the thrust piston contribution) as a function of the compressor end pressure, p_{out}. Two different linear trends are found, depending on the fact that IGV are partly closed (left hand side line) or fully opened (right hand side line). Furthermore, with closed IGV, the load relief is lower of about 15% with respect to fully opened IGV condition. Note that varying IGV position, from closed position to maximum opening, produces an increase of compressor mass flow, $\dot{m}$, from 62.5%, with respect to base load reference condition $\dot{m}_0$, to 102,5%.

Then, results point out that the axial thrust on the compressor bearing, *BT*, is not only a function of the compressor end pressure, but depends also on ambient temperature and IGV opening. This is a consequence of the compressor pressure state line, which varies with room temperature and IGV opening degree, as shown in Figure 14. Basically, when the compressor operates in extreme off-design conditions (closed IGV and/or low ambient temperature), the pressure level at the first extraction point, that supplies the thrust piston (5th compressor stage), suffers a strong decrease with respect to the compressor end pressure.

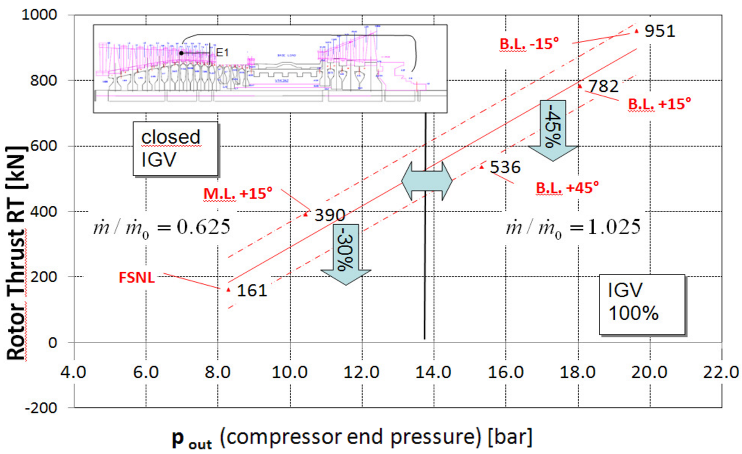

Figure 12 – Rotor axial thrust vs. compressor end pressure for AE94.3A gas turbine.

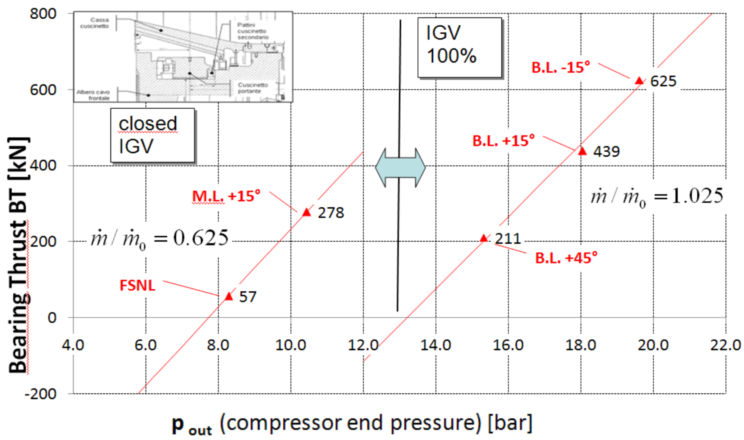

Figure 13 – Axial bearing load vs. compressor end pressure for AE94.3A gas turbine.

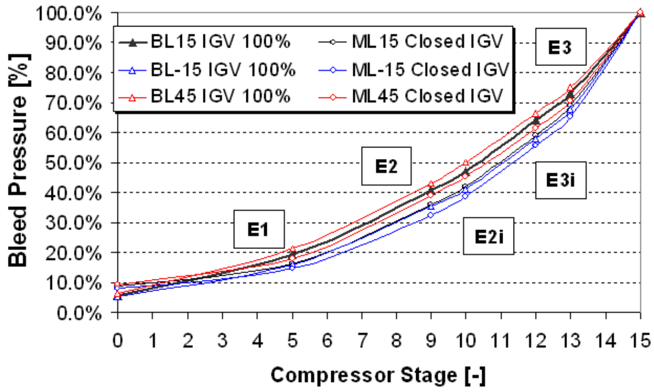

Figure 14 – Compressor pressure lines for AE94.3A GT.

RAT CODE VALIDATION

In order to validate the RAT code, comparison of calculation results with experimental data was carried out for AEx4.3A and AE94.2 gas turbines, in base load condition at different room temperature and in off design conditions. The calculation procedure was adjusted to fit experimental data. In particular, for each gas turbine model, mentioned calibration coefficients for pressure values in the Set-up file (Figure 7) were used, in order to match experimental data in the base load reference condition (BL15). The same set of calibration coefficients was then applied to the other operating conditions showing a good agreement with experimental data.

Measurement system

The measurement system for typifying the main thrust bearing and tuning the code should consist of, at least, 2 load cells and 1 proximity probe (Figure 15). In addition, from the GT standard monitoring system, power output and rotational velocity should be acquired at the same time. The load cell measures the thrust value on a single pad. The proximity probe measures the distance variation between the pads and the rotor, which corresponds to the oil thickness [10], and it allows evaluating the rotor movement during start-up and shut-down phases.

The proximity probes can be installed in front of the GT coupling flange, on a customized support fixed on the bearing hat. The cable is usually passed on the bearing surface, fixed on the protection cone and passed out the bearing house to the signal conditioner.

The load cells can be previously installed by the bearing supplier or directly in the workshop before the GT assembly. The load cells are located on the spring element of the thrust bearing. Cables for cells could be passed on the bearing surface, fixed on the protection cone and passed out the bearing house to the signal conditioner.

In case of two cells, the instrumentation should be installed near the center line on the two opposite hand-sides (red circles shown in Figure 4). This is in order to prevent inequality of bearing load in the tangential direction (more details about bearing design are given in [11]). Such load differences are due to several factors: non perfect shaft alignment during operation, bearing tolerances, different stiffness and irregular heating of upper and lower part of the casing, etc.. Using two cells, the whole thrust can be calculated by averaging the values of the two probes and multiplying for the number of pads. The resulting scatter band of two load cells usually is of the order of ±10%. Moreover, measured values often show fluctuations that must be filtered out during data post-processing. Dynamic bearing loading may be influenced by different factors such as bearing tolerances.

Errors of bearing load measurements are due to measurement system components errors. The measurement chain is composed by: load cell; signal conditioner; cables and data acquisition system. The estimated error of the measurement system is 5%.

Note that:

- In order to monitor the possible negative thrust during the initial part of the start-up phase, secondary bearing pads should be instrumented as well.
- For accuracy of measured thrust and to improve the code validation, a great number of thrust pads could be monitored, and an additional proximity probe could be installed in front of the flange.
- In data analysis, consider misunderstanding due to the occasional deformation of the bearing-rotor system.

Further data can be acquired in order to complete the measurement system for RAT validation, namely:

- pressure level in the thrust piston (see *calibration coefficients* paragraph).
- Temperatures of pads (to investigate inequality of load and oil thickness in the tangential direction, see [10]).

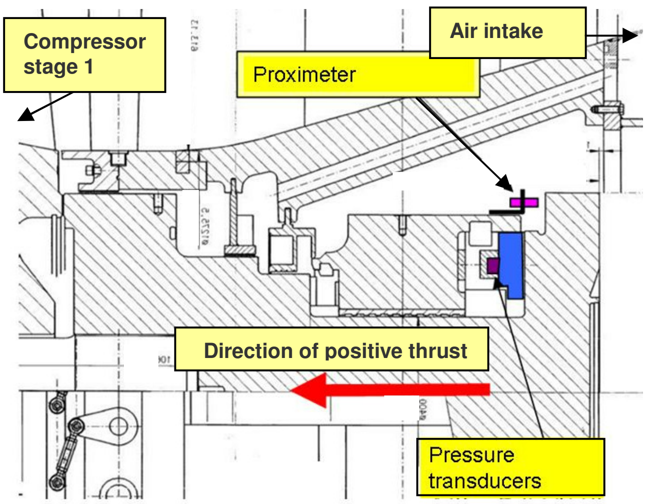

Figure 15 – Measurement locations on the fore shaft.

Discussion of experimental results

In test campaigns on AE94.3A and AE94.2 gas turbines, here described, load cells were installed on the main thrust bearing. Furthermore, a proximity probe was used to monitor the distance between the bearing casing and the rotor. Since only the main thrust bearing was equipped with load cells, for the first part of the start-up phase (roughly until 20% of rated speed is reached) axial load on the working bearing (the secondary one) is not available. However for AE94.2, the contemporary acquisition by load cell and proximity probe, in dependence with rotational speed (shut on – shut down) and acquisition time t (partial load – full load), allows knowing the direction of axial thrust.

Figure 16 and 17 show the measurements of three load cells and of a proximity probe on the main bearing of AE94.2 TG. To clarify the temporal evolution of measured data, rotational speed is reported (Figure 18). Proximity sensor measurements (Figure 17) show that during initial start-up the axial thrust is directed towards the compressor inlet, thus loading the secondary bearing. In fact, as already pointed out, during initial start-up, from 0 to 1750 RPM, the axial thrust on compressor section is typically higher than the one on the turbine section, thus leading to a net balance of axial thrust directed towards the compressor inlet.

Note that, since only the main bearing thrust was equipped with load cells, load measurements are valid only above 1750RPM. Hence the first part of Figure 16 must not be considered.

After ignition (1750 RPM) the axial thrust starts to increase, and is directed towards the turbine exhaust diffuser. At the nominal rotational speed the pads load attains constant values.

Figure 16 also shows that the load distribution on bearing pads is not uniform. With respect to the axial load measured by each pressure transducer at nominal speed, a scatter band of ≈ ±10% occurs, which is mainly due to a non perfect longitudinal alignment of the rotor, as already discussed.

In order to summarize in a single graph the main conclusions of calculation results and experimental data for different gas turbines, values of the main axial bearing thrust and compressor end pressure were scaled with the reference value in BL15 conditions. The summary of main results is shown in Figure 20. Calculated and measured points show quite a good agreement, in particular with fully opened IGV. Note that the extreme off-design condition BL-15 calculated for AE94.3A is less significant than other points, since gas turbine IGV usually start closing when ambient temperature drops below 0°C.

Results confirm that the IGV opening degree drives two different trends of axial thrust with compressor end pressure. In base load condition, with IGV fully opened, AE64.3A, AE94.3A and AE94.2 show a similar behavior, as pointed out by the overlap of the interpolating lines. On the other hand, with IGV partly closed it's not possible to gather experimental data of different TG on a single interpolating line. This is not surprising, since each of the investigated gas turbines has a completely different compressor technology and a strongly different level of turndown load. As a consequence, with IGV partly closed they behave in a much different way.

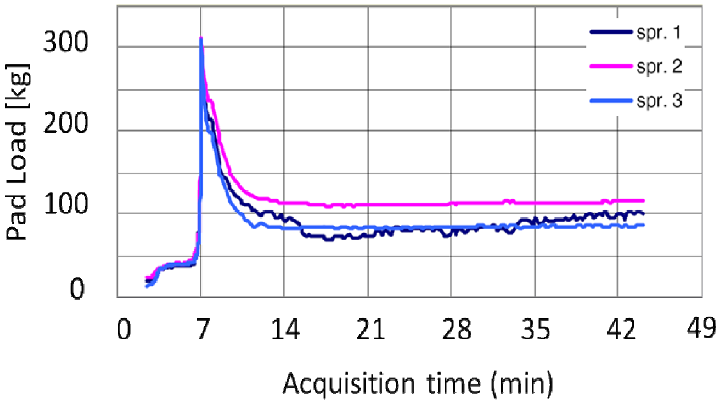

Figure 16 – Pressure transducers measurements during start-up for AE94.2 gas turbine.

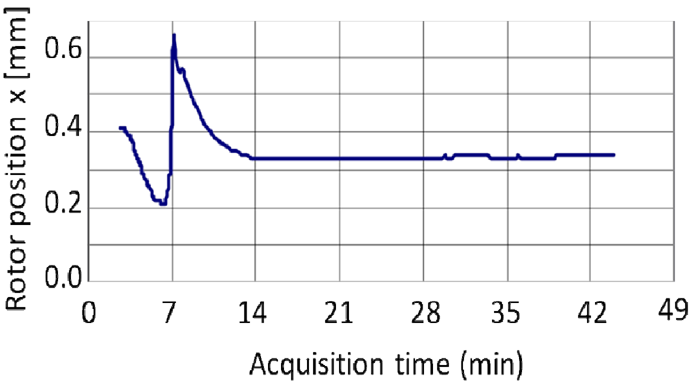

Figure 17 – Relative movement between rotor and bearing casing during start-up for AE94.2 gas turbine.

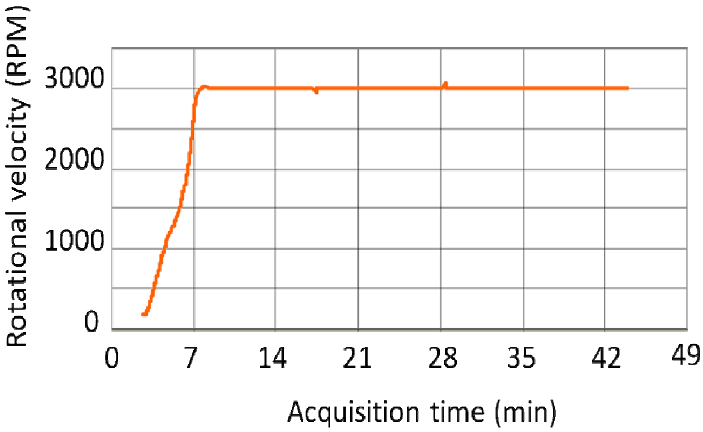

Figure 18 – Rotational speed during start-up for AE94.2 gas turbine.

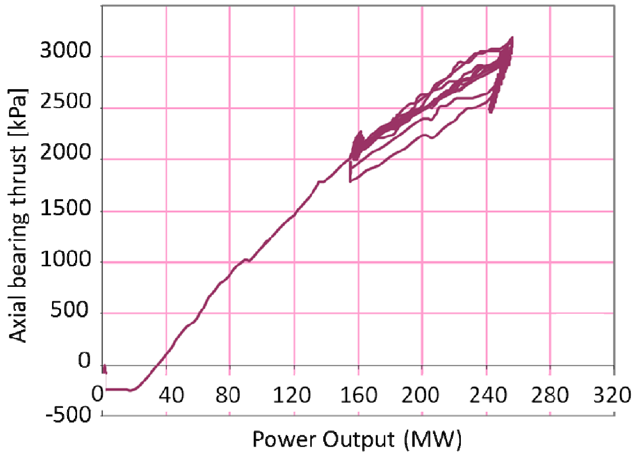

Figure 19 - Bearing load as a function of power output for AE94.3A gas turbine

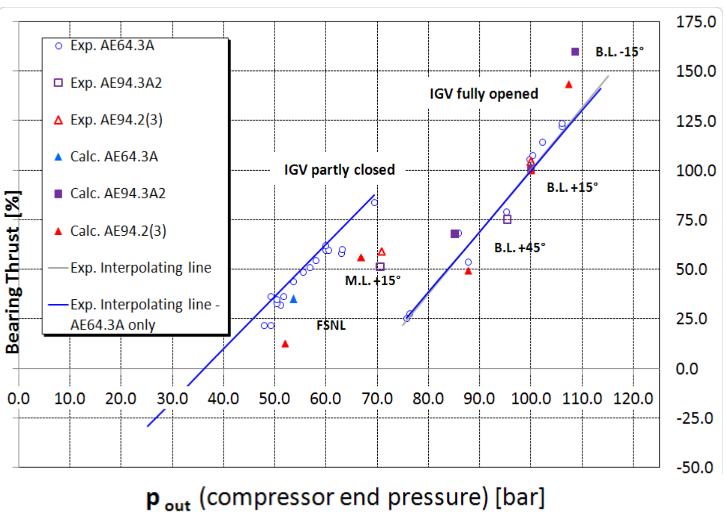

Figure 20 – Axial bearing load as a function of compressor discharge pressure (summary of calculated and measured points for AEx4.3a and AE94.2 GTs).

Fitting of bearing load data

A calculation campaign for different TG in varying operating conditions was performed, in order to build correlations for the rotor axial thrust and the bearing thrust. Calculation results were validated with experimental data previously discussed.

The analysis suggests that, in the whole range of operating conditions, the rotor thrust RT grows linearly with the pressure level of the gas turbine engine, according to the law:

$$RT = k \cdot p_{out} - z \qquad [1]$$

where p_{out} represents the compressor end pressure and k is the rotor thrust gradient in [kN/bar].

The parameters k and z in Eq. [1] were evaluated, for each gas turbine investigated, by means of a linear regression of the calculated data points, based on the Ordinary Least Squares approach. Table 2 shows the values of the parameters k and z for different gas turbine sizes.

Model	Power [MW]	P.R.	k [kN/bar]	z [kN]
AE94.3A	294	18.2	90	800
AE94.2	170	12	50	250
AE64.3A	75	16.7	30	150

Table 2 – Rotor thrust gradient and off-set coefficient for Ansaldo gas turbines.

Similarly to the rotor thrust RT, the axial bearing thrust, *BT*, can still be expressed as a linear function of the pressure level of the engine, defined by the compressor end pressure p_{out}:

$$BT = m \cdot p_{out} - c(IGV) \qquad [2]$$

The term m represents the bearing thrust gradient (bearing thrust versus compressor end pressure, [kN/bar]) and it is, similarly to the coefficient k in Eq. [1], approximately constant for a TG of given class and size. Conversely, as already pointed out by Figure 13 and 20, the coefficient c in Eq. [2] is not a constant but it depends on the IGV opening, thus on the $\dot{m}/\dot{m}_0$ ratio.

Similarly to the terms in Eq. [1], the *m* coefficient was evaluated, for each gas turbine investigated, by means of a linear regression of the calculated data points, based on the Ordinary Least Squares approach. Table 3 shows the values of the coefficient *m* calculated for different gas turbine sizes.

Model	Power [MW]	P.R.	m [kN/bar]
AE94.3A	294	18.2	100
AE94.2	170	12	90
AE64.3A	75	16.7	30

Table 3 – Bearing Thrust gradient and off-set coefficient for Ansaldo gas turbines.

CONCLUSIONS

A numerical tool for calculation of rotor axial thrust of heavy duty gas turbines has been presented. RAT code acquires geometry data, pressure values along the rotor and compressor/turbine blades thrust, and it returns the rotor thrust as well as the net load on the main and secondary bearings.

In order to validate the code, comparison of calculated thrust with experimental data was carried out for AEx4.3A and AE94.2 gas turbines, in base load condition at different room temperature and in off design conditions.

Calculations, as well as field measurements, show that rotor axial thrust grows linearly with the pressure level of the gas turbine. On the other hand, the main axial bearing load, plotted as a function of compressor end pressure, shows two different linear trends depending on the fact that IGV are partly closed or fully opened.

Experimental data recorded by a proximity sensor measuring the rotor position with respect to bearing case, point out that axial thrust is always directed towards the turbine exhaust diffuser, except for a short period of time during start-up, when the axial thrust is directed towards the compressor air intake.

REFERENCES

1. B. Becker, 2002, "Robust gas turbine design", ASME paper no. GT2002-30159.
2. Reichert A.W., Janssen M. 1996, "Cooling and sealing air system in industrial gas turbine engines", ASME paper GT-256.
3. Brillert D., Reichert, A.W., Simon, H., 2001, "The flow structure in rotating hollow shafts in radial inflow and axial through flow", ASME 2001-GT-203.
4. Brillert D., Mirzamoghadam A.V., Dohem H.J., 2003, "Application of conjugate CFD to the internal cooling air flow system of gas turbine," ASME GT-38471.
5. G. Vermes, 1961, "A fluid mechanics approach to the labyrinth seal leakage problem", ASME Journal of engineering for power, April, 1961, pag. 161.
6. Bianchini C., Da Soghe R., Facchini B., Innocenti L., M. Micio, 2008, "Development of a Numerical Tool for Stator-Rotor Cavities Calculation in Heavy-Duty Gas Turbines", IGTI ASME Cogen Turbo Power Congress.
7. Bozzi L., Luccoli R., Sacchetti M., Traverso S., 2004, "CFD investigation of the internal cooling air flow system of heavy-duty gas turbines", 59° ATI, Genoa, 2004.
8. Reichert A.W., Brillert D., Simon H., 1998, "Cooling air flow in a multi disk industrial gas turbine rotor", ASME paper GT-136
9. Bonzani F., Bozzi L., Mantero M., Vinci A., Innocenti L., Micio M., 2010, "1D tool for stator-rotor cavities integrated into a fluid network solver of heavy-duty gas turbine secondary air system", ASME paper 22203
10. N. H. New, "Experimental comparison of flooded directed, and inlet orifice type of lubrification for a tilting pad thrust bearing", AT 406/74.
11. Martin F. A., "Tilting pad thrust bearing: rapid design aids", The Institution of Mechanical engineers, Tribology Convention, 1970.

ACKNOWLEDGEMENTS

The authors would like to acknowledge the help of Mr. Rebizzo Adelmo for the handling of experimental results.